

3-D FINITE ELEMENT SIMULATION OF PULSATING FREE BULGE HYDROFORMING OF TUBES*

M. LOH-MOUSAVI^{1, **}, M. BAKHSHI², K. MORI³, T. MAENO³, M. FARZIN⁴ AND S.J.
HOSSEINIPOUR²

¹Dept. of Mechanical Engineering, Islamic Azad University (Khomeinishahr Branch), I. R. of Iran
Email: loh-mousavi@iaukhsh.ac.ir

²Dept. of Mechanical Engineering, Mazandaran University, I. R. of Iran

³Dept. of Production Systems Engineering, Toyohashi University of Technology, Japan

⁴Dept. of Mechanical Engineering, Isfahan University of Technology, Isfahan, I. R. of Iran

Abstract– Application of pulsating pressure is a new and effective method to improve the formability of the tube hydroforming process. However, the factors that cause this improvement are still unclear. In this paper, the forming mechanism of pulsating free bulge hydroforming of tubes is studied using both finite element simulation and experiment. The effects of oscillating pressure on deformation behavior, thickness distribution, strain path and friction force are examined. It is shown that for a constant pressure path, the wall thickness decreases quickly up to bursting; whereas for the pulsating pressure, the thickness decreases gradually, and thus, local thinning is prevented by oscillating internal pressure. Formability is improved due to an increase of the longitudinal compressive strain and better wrinkling behavior. Small harmonic wrinkles appear and are removed during the pulsating process, hence, by this mechanism bursting and wrinkling are prevented, causing improvement of formability.

Keywords– Tube, finite element method, free bulge hydroforming, pulsating hydroforming, formability

1. INTRODUCTION

Tube hydroforming technology is an innovative metal forming process that is generally used to form complex hollow parts from tubular specimens. In recent years, this process has grown due to its capabilities in decreasing production costs and in optimizing production technology. In particular, this technique has attracted the attention of the automotive industry due to the reduction in weight of automotive parts [1].

In the hydroforming process, to manufacture a part with no defects and with the required dimensional tolerances, proper application of the internal pressure path is very important [2]. An effective path for improving the formability in this process is known as pulsating pressure path [3]. For a monotonic internal pressure, wrinkling and bursting are caused by small and large pressures, respectively; whereas these defects are prevented by the oscillation of internal pressure in the pulsating hydroforming. In this process, the internal pressure required to form the tube is oscillated during the axial feeding.

During the last decades, finite element (FEM) simulations of metal forming processes have become important tools for designing and optimizing feasible production processes [4, 5]. Mori et al. [6, 7] have simulated the axi-symmetric pulsating hydroforming of tubes by rigid-plastic finite element method. Hama et al. [8] have exhibited the effectiveness of the oscillation of internal pressure on the formability for an automotive part by the static explicit finite element method. The authors have studied the effect of

*Received by the editors May 14, 2007; Accepted November 1, 2008.

**Corresponding author

oscillation of internal pressure on the formability and geometrical accuracy of the products in the pulsating hydroforming process for T-shaped parts using a dynamic explicit finite element code [9]. The authors have also proposed a new method to improve die corners filling in box-shaped tube hydroforming by controlling wrinkling and under oscillation of internal pressure [10].

Since the frequency of the ultrasonic vibration is much higher than the pulsating hydroforming, it is likely that the latter may have a different mechanism for improving the formability as compared with the former [11]. The factors that improve the formability in pulsating tube hydroforming are still unclear and fundamental studies about these factors are scarce. In this paper, the pulsating free bulging process has been further studied by the three dimensional dynamic explicit finite element method. Effects of oscillating internal pressure on the deformation behavior, thickness distribution, strain path and friction force are examined. In addition, the results of finite element simulation are compared with experimental data.

2. EXPERIMENTATION

To examine the effect of pulsating pressure on deformation behavior, free bulging experiments were carried out. Figure 1 shows the tools and tube used in the experiments. A computer controlled hydraulic machine was employed to generate the pressure paths shown in Fig. 2. A water-oil emulsion was used as a pressure media and machine oil was used as a lubricant in the experiment.

The die-set shown in Fig. 1 was used to measure the friction force in the hydroforming process. Since it is not easy to measure the friction force over all the interfaces during the hydroforming, only the friction force in the feeding zone of the tube was obtained. The tooling is composed of the upper and lower dies, the upper and lower punches, and the load cell. The load cell was used to measure friction force in the feed zone between the upper die and the tube. The tube is pushed by the upper punch downward against the lower punch. The punch force was also measured during the experiments. The ram speed was set at 90 mm/min. The diameter, wall thickness and length of the mild steel tube were 38.4 mm, 1.1mm and 200 mm, respectively.

The pulsating and peak pressure paths shown in Fig. 2 were set to examine the effect of oscillating pressure during the hydroforming process. The pulsating pressure was oscillated from the mean pressure (17.5 MPa) with an amplitude of 3 MPa and with a frequency of 0.67 cycles/mm. The peak pressure path is a constant pressure equal to the maximum value of pulsating pressure.

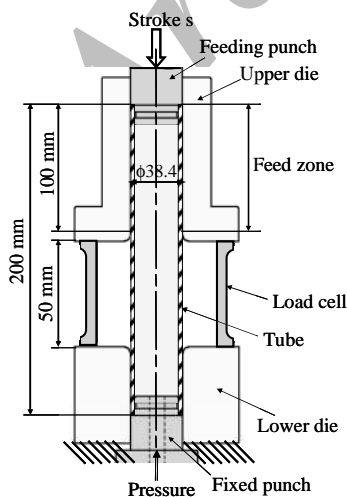


Fig. 1. Tools and tube used for experiments

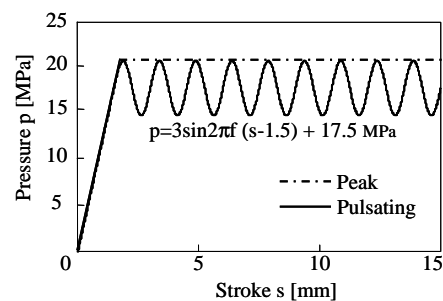


Fig. 2. Two pressure paths used for experiment

3. FE SIMULATION

To simulate the hydroforming process, ABAQUS explicit code was used. As shown in Fig. 3, only half of the tube was modelled due to symmetry and rigid tools were assumed in the simulations. The penalty contact approach was employed for the contact between the tube and die. The position of the weld line was considered to be on the symmetric plane, as is shown in the figure.

The tube and tools were meshed with 1200 3D shell elements. The tube material data used in the finite element simulation are given in Table 1. The flow stress and r-value of the mild steel tube were measured by the tensile test. The flow stress of the weld line of the tube was also measured by the tensile test and used in the simulation as shown in Table 2. The coefficient of friction, μ , was approximately 0.015, and was calculated based on the experiments and using the Coulomb equation, $\mu = F_f / F_N = F_f / (P \times A)$. In this equation P is the contact pressure (the average internal pressure), A is the contact area (area of the feed zone between the tube and upper die), and F_f and F_N are the measured friction force and the normal contact force between the tube and upper die at the same stroke, respectively.

The Hill's anisotropic yield criterion was employed in the finite element simulation. The velocity of the upper punch and the pressure paths were defined based on the experimental data. In this simulation, the mass-scaling approach was used in the explicit dynamic finite element simulation to reduce the computation time. The effect of mass-scale value on the kinetic energy was checked to ensure that the kinetic energy is less than 5% of total strain energy.

Table 1. Material properties of tube used in the finite element simulation

Young's modulus	210 GPa
Poisson's ratio	0.3
Yield stress	280 MPa
Flow stress	$\sigma = 510\epsilon^{0.12}$ MPa
Coefficient of friction	0.05
R-Value	1.6

Table 2. Material properties of tube weld line used in the finite element simulation

Yield stress	321 MPa
Flow stress	$\sigma = 523\epsilon^{0.1}$ MPa

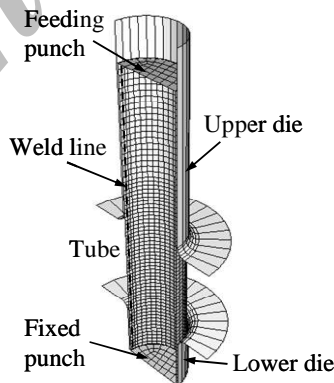


Fig. 3. Finite element model used for simulation

4. RESULTS AND DISCUSSION

a) Geometry

The geometries of the formed parts are shown in Fig. 4. For the peak pressure (constant pressure), round bulging occurred during the process, while a flat shape bulging appeared for the pulsating pressure.

The deformation behavior of the tube at various strokes during the free bulge hydroforming is shown in Fig. 5. It can be observed that while the tube is fed, in each oscillation a few wrinkles appear when the pressure is low; and when the pressure increases, wrinkles disappear. This phenomenon is repeated for each cycle during the pulsating hydroforming causing a flat shape bulging. In other words, this small growth of wrinkles for the pulsating hydroforming is not necessarily a defect, since these wrinkles can be removed by increasing the inner pressure in each cycle of oscillation. It will be shown in the next section that this deformation behavior increases the formability by prevention of bursting.

The simulated cross-sectional shapes of the deformed tube for the peak and pulsating pressures are compared with the experimental results in Fig. 6. It is seen that the results are in close agreement.

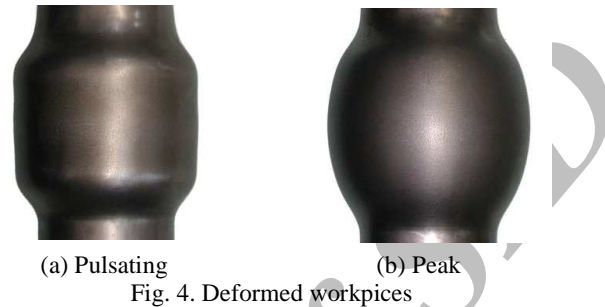


Fig. 4. Deformed workpieces

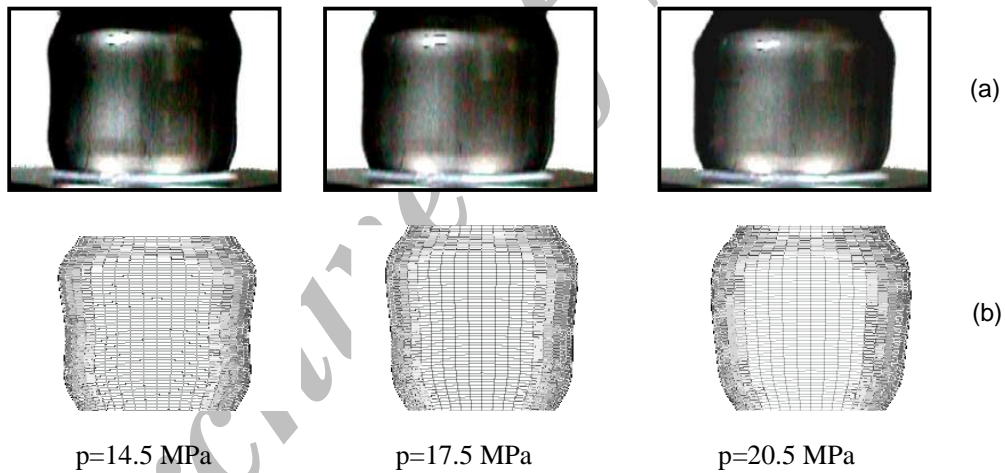


Fig. 5. Deformation behaviour of the tube at different strokes during the pulsating hydroforming process, (a) Experimental, (b) Simulation

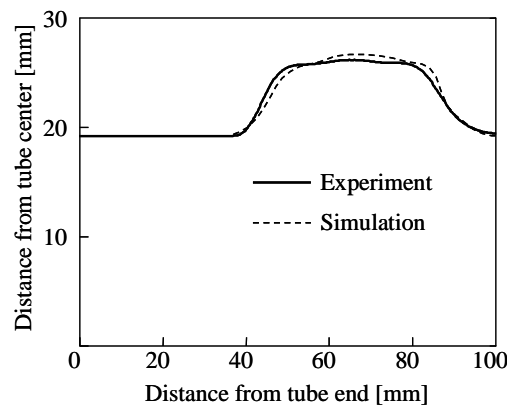


Fig. 6. Cross sections of the deformed tube for $s=15\text{mm}$, obtained from experiment and simulation

b) Thickness distribution

Wall thickness distributions for pulsating tube hydroforming obtained from FEM simulation and experiment are shown in Fig. 7. It is seen that the results are in good agreement.

Calculated wall thicknesses at the center of the protrusion versus stroke are compared with the experimental ones in Fig. 8 for the peak and pulsating pressures. For the peak pressure, the thickness decreases quickly up to bursting; whereas the wall thickness decreases gradually for the pulsating pressure.

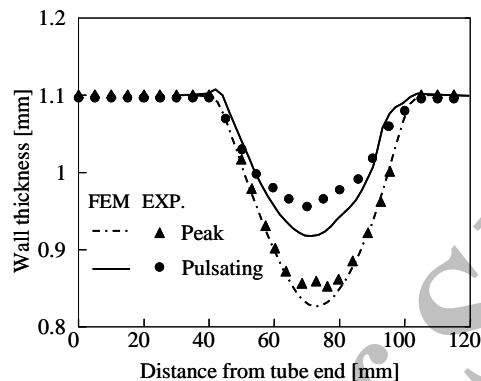


Fig. 7. Wall thickness distribution of the tube for the pulsating pressure obtained from experiment and FE simulation

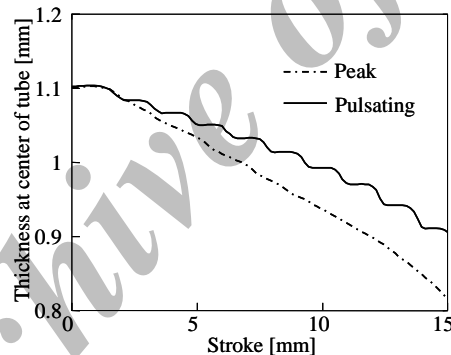


Fig. 8. Variations in wall thickness at the center of protrusion during hydroforming obtained from FE simulation

c) Friction force and contact pressure

Figure 9 illustrates the variations of friction force in the feed zone for the two pressure paths obtained from experiments and FE simulations. In general, it can be observed that, for the pulsating pressure, the friction force is not much smaller than that for the constant pressure. On the other hand, the friction forces obtained from simulations are smaller than the experimental ones. This is mainly due to two reasons. Firstly, in the evaluation of the coefficient of friction, a uniform contact pressure was considered for the whole area of the feed zone. Figure 10 shows the deformed tube in the pulsating hydroforming. The galling occurs near the top corner of the upper die and at the end of the feed zone, while there is no galling in the middle region of the feed zone. This means that the contact between the tube and upper die is not uniform. Thus it is likely that a small coefficient of friction has been obtained because a larger contact area has been assumed. Secondly, and more importantly, the contact pressure was approximated by the internal pressure, leading to larger pressures and a smaller friction coefficient as compared with actual ones.

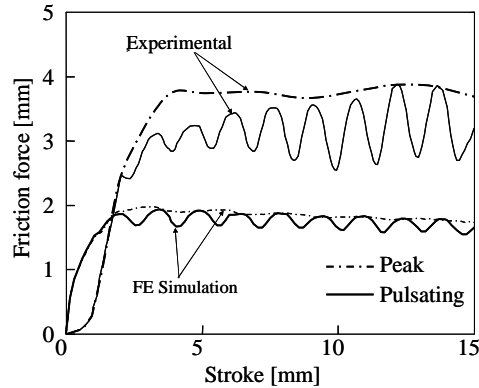


Fig. 9. Measured friction force by experiment for pulsating and constant pressure

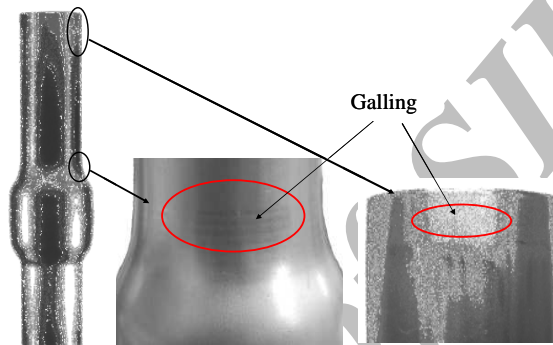


Fig. 10. Deformed tube and the selections of tube in contact with top and bottom ends of upper die

d) Strain distribution along the axial direction of the tube

In sheet metal forming, failures are related to the material formability and these phenomena are difficult to quantify since they depend on the material used and the stress and strain states imposed on the workpiece. Therefore, stress or strain states should be considered as key parameters to study the deformation behavior of the tube. The simplest available method for the evaluation of sheet metal formability is using the forming limit curves (FLC). These curves are commonly used to check whether the strains exceed the material's forming capacity or not. FLCs are mostly constructed from the data obtained by several experiments with different linear strain paths. Since formability is strongly dependent on the deformation history, experimental determination of the FLCs is difficult. Therefore in practice, FLCs are often determined from analytical expressions or from FE simulations.

In this study, FLCs are used to examine the effect of pulsating pressure in the free bulge hydroforming process. Figure 11 shows the major (ϵ_1) and minor (ϵ_2) strains of the bulged tubes obtained from the FE simulation. The forming limit diagram obtained by Ref. [12] for an STKM-11A tube, is also shown in the diagram. It is found that the major strains occurring near the center of the tube for the pulsating pressure are smaller than those for the peak pressure.

e) Strain path

To see the effect of the pulsating pressure on the deformation process, strain path at the center of the deformed tube is studied by the finite element method. The results are compared for the pulsating and constant peak pressures in Fig. 12.

It can be observed that for the pulsating pressure, longitudinal compressive strain is more than constant pressure. This means that better end feeding can be performed, and as a result, the thinning

decreased as shown in Fig. 8. In other words, by improvement of axial feeding, longitudinal compressive strain increases, which can increase the tube wall thickness.

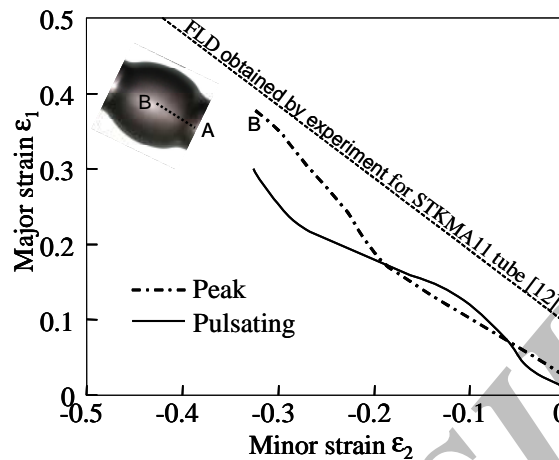


Fig. 11. Strain distribution along the axial direction of tube obtained from finite element simulation

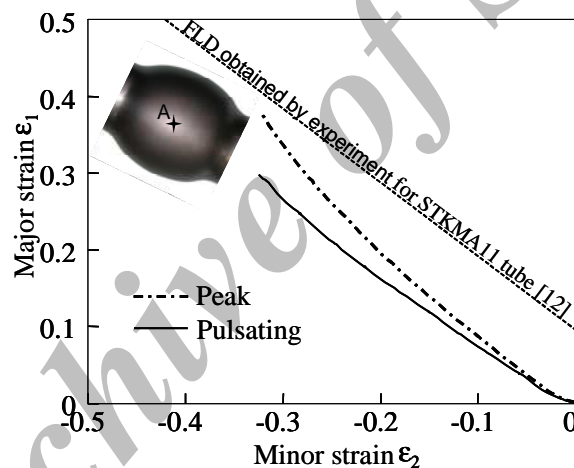


Fig. 12. Strain paths on the center of deformed tube

5. CONCLUSION

In this paper, the effect of pulsating pressure on free bulging tube hydroforming was studied, both numerically and experimentally. The value of coefficient of friction was measured experimentally and modified by the finite element simulation. Based on the modified value of friction coefficient, variations of friction force, thickness distribution and geometry of the formed part were calculated and compared to the experimental results. It is shown that the results are in good agreement.

It is also shown that the wall thickness of the tube decreases gradually for the pulsating pressure; whereas for the same non-pulsating peak pressure path, the wall thickness decreases more quickly up to bursting, due to different bulging deformation during the hydroforming process. In addition, the effect of pulsating pressure on the strain path of the tube center was studied by the finite element method. It was found that the bursting can be postponed by pulsating pressure, due to the increase of the longitudinal compressive strain. The increase of longitudinal compressive strain was achieved by the improvement of the material end feeding.

REFERENCES

1. Mac Donald, B. J. & Hashmi, M. (2002). Near-net-shape manufacture of engineering components using bulge-forming process. *J. Mater. Process. Technol.*, Vol. 120, pp. 341-347.
2. Koc, M. & Altan, T. (2002). Prediction of forming limits and parameters in the tube hydroforming process. *Int. J. of Mach Tools and Manuf.*, Vol. 42, pp. 123-138.
3. <http://www.opton.co.jp>.
4. Moslemi Naeini, H., Kiuchi, M., Shintani, K., Kitawaki, T. & Kuromatsu, R. (2003). A new design method of rolls for reshaping process of non-circular pipes. *Iranian Journal of Science & Technology, Transaction B, Engineering*, Vol. 27, No. B3, pp. 521-533.
5. Moslemi Naeini, H., Maerefat, M. & Soltanpour, M. (2005). Finite element simulation of hot forming process by using flow stress prediction model. *Iranian Journal of Science & Technology, Transaction B, Engineering*, Vol. 29, No. B2, pp. 231-240.
6. Mori, K., Maeno, T. & Maki, S. (2006). Mechanism of improvement of formability in pulsating hydroforming of tubes. *Int. J. of Mach Tools and Manuf.*, Vol. 47, pp. 978-984.
7. Mori, K., Patwari, A. U. & Maki, S. (2004). Improvement of formability by Oscillation of Internal pressure in pulsating hydroforming of Tube. *Annals of the CIRP*, Vol. 53, No. 1, pp. 215-218.
8. Hama, T., Asakawa, M., Fukihara, H. & Makinouchi, M. (2003). Finite element simulation of hammering hydroforming of an automotive component. *Proc. of the TUBEHYDRO 2003*, Aichi, Japan, pp. 80-83.
9. Loh-Mousavi, M., Mori, K., Hayashi, K., Maki, S. & Bakhshi, M. (2007). 3-D finite element simulation of pulsating T-shape hydroforming of tubes. *Key Eng. Mater.*, Vol. 340, pp. 353-358.
10. Loh-Mousavi, M., Mori, K., Hayashi, K. & Bakhshi, M. (2007). Improvement of filling of die corners in box-shaped tube hydroforming by control of wrinkling. *Key Eng. Mater.*, Vol. 344, pp. 461-467.
11. Mori, K., Maeno, T., Bakhshi-Jooybari, M. & Maki, S. (2005). Measurement of friction force in free bulging pulsating hydroforming of tubes. in: P.F. Bariani et al. (Ed.), *Advanced Technology of Plasticity 2005*, Edizioni Progetto Padova, Padova, 2005, CD-ROM.
12. Kim, J., Kim, S. W., Song, W. J. & Kang, B. S. (2005). Analytical and numerical approach to prediction of forming limit in tube hydroforming. *Int. J. of Mechanical Sciences*, Vol. 47, pp. 1023-1037.